Atmos. Chem. Phys. Discuss., 9, 15641–15671, 2009
www.atmos-chem-phys-discuss.net/9/15641/2009/
© Author(s) 2009. This work is distributed under
the Creative Commons Attribution 3.0 License.

Atmospheric Chemistry and Physics Discussions

This discussion paper is/has been under review for the journal *Atmospheric Chemistry and Physics (ACP)*. Please refer to the corresponding final paper in *ACP* if available.

High levels of reactive gaseous mercury observed at a high elevation research laboratory in the Rocky Mountains

X. Faïn[1], D. Obrist[1], A. G. Hallar[1,2], I. McCubbin[1,2], and T. Rahn[3]

[1]Division of Atmospheric Sciences, Desert Research Institute, 2215 Raggio Parkway, Reno, NV, USA
[2]Storm Peak Laboratory, Desert Research Institute, P.O. Box 882530 Steamboat Springs, CO, USA
[3]Earth and Environmental Sciences Division, Los Alamos National Laboratory, P.O. Box 1663 Los Alamos, NM, USA

Received: 15 April 2009 – Accepted: 2 June 2009 – Published: 24 July 2009

Correspondence to: X. Faïn (xavier.fain@dri.edu)

Published by Copernicus Publications on behalf of the European Geosciences Union.

Abstract

The chemical cycling and spatiotemporal distribution of mercury in the troposphere is poorly understood. We measured gaseous elemental mercury (GEM), reactive gaseous mercury (RGM) and particulate mercury (Hg_P) along with CO, ozone, aerosols, and meteorological variables at Storm Peak Laboratory at an elevation of 3200 m a.s.l., in Colorado, from 28 April to 1 July 2008. The mean mercury concentrations were 1.6 ng m^{-3} (GEM), 20 pg m^{-3} (RGM) and 9 pg m^{-3} (Hg_P). We observed eight events of strongly enhanced atmospheric RGM levels with maximum concentrations up to 135 pg m^{-3}. RGM enhancement events were unrelated to daytime/nighttime patterns and lasted for long time periods of 2 to 6 days. During seven of these events, RGM was inversely correlated to GEM (RGM/GEM regression slope ~ -0.1), but did not exhibit correlations with ozone, carbon monoxide, or aerosol concentrations. Relative humidity was the dominant factor affecting RGM levels with high RGM levels always present whenever relative humidity was below 40 to 50%. We conclude that RGM enhancements observed at Storm Peak Laboratory were not induced by pollution events and were related to oxidation of tropospheric GEM, but the mechanism remain unclear. Based on backtrajectory analysis and a lack of mass balance between RGM and GEM, we propose that in situ production of RGM may have occurred in some distance allowing for scavenging and/or deposition of some RGM prior to reaching the laboratory, and that GEM oxidation is an important tropospheric Hg sink. Our observations provide evidence that the tropospheric pool of mercury is frequently enriched in divalent mercury and that high RGM levels are not limited to the upper troposphere.

1 Introduction

Mercury is a worldwide pollutant globally dispersed in the environment by large-scale atmospheric circulation. Various natural and anthropogenic sources emit mercury to the atmosphere, either as gaseous elemental mercury (GEM; Hg^0) or as divalent

mercury species. Divalent mercury species are typically measured in two forms: reactive gaseous mercury (RGM), defined operationally as any gaseous mercury compounds that adsorb onto KCl (potassium chloride) denuders, and particulate-bound mercury (Hg_P) which are trapped by quartz-fiber filters. RGM is water-soluble, and can be rapidly deposited to surfaces when sequestered by rain or cloud drops (Schroeder and Munthe, 1998). Hg_P is limited to the lifetime of particles which is typically less than 10 days (Schroeder and Munthe, 1998). Contrarily, GEM has low solubility in water and estimates of its longer lifetime range from 0.5 to 2 years (Schroeder and Munthe, 1998; Bergan and Rodhe, 2001; Selin and Jacob, 2008), although GEM lifetime is still not well understood. Hence, the speciation of atmospheric mercury and, specifically, the abundance of reactive mercury forms with high deposition velocities, are of utmost importance for regional and local deposition loads and for the understanding of global chemical cycling of mercury in the atmosphere.

Many atmospheric observations have been conducted in the lower troposphere where GEM generally represents over 95% of the total mercury, with concentrations varying over a range of ~1–5 ng m^{-3} (Valente et al., 2007), and RGM and Hg_P in the range of few percent of the total mercury (Schroeder and Munthe, 1998). The vast majority of measurements of atmospheric mercury species have been conducted at ground-level, and these low altitude data suggest that little RGM and Hg_P is present distant from sources. Recent aircraft campaigns over the Pacific, however, indicated a strong depletion of GEM in the upper troposphere and lower stratosphere, which is hypothesized to be due to efficient oxidation and transformation of GEM to RGM and Hg_p (Friedli et al., 2004; Radke et al., 2007; Talbot et al., 2007; Slemr et al., 2009). Interestingly, global chemical model showed that divalent mercury species could dominate GEM in the upper troposphere and stratosphere, and that subsidence could be a significant source of divalent mercury to remote surface sites (Sillman et al., 2007; Selin and Jacob, 2008). Direct measurements of RGM and Hg_P onboard of aircraft are presently not available, due to the long collection period required (2–3 h using the 1130 and 1135 Tekran units, see Materials and Methods). In situ measurements of

aerosols collected in the lower stratosphere and analyzed using mass spectrometry indicate, however, significant enrichment of Hg_P (Murphy et al., 2006). At a high elevation (2700 m a.s.l.) research station, Mt. Bachelor observatory in Oregon, USA, decreases of GEM and enhanced levels of RGM were observed frequently at night when the air was considered representative of the free troposphere (Swartzendruber et al., 2006). The authors suggested in situ oxidation of GEM by ozone, OH, or possibly other oxidants in the free troposphere as sources of RGM, which then could reach the laboratory during nighttime downflow processes (i.e., katabatic winds) induced by the mountain slopes.

The dearth of reactive mercury observations in the upper troposphere and the first observational and modeling results emphasize the need for increased measurements of reactive mercury in this region. Such data would improve our understanding of temporal and spatial distribution of all forms of mercury and of atmospheric mercury chemistry, and thus help to reduce uncertainties in model simulations. We report data of speciated atmospheric mercury levels at a high-altitude research station, Storm Peak Laboratory (3220 m a.s.l.) in the Rocky Mountains in Colorado, from 28 April to 1 July 2008 to study the presence and transformation of reactive mercury in the troposphere over the remote Western United States.

2 Material and methods

2.1 Site description

Storm Peak Laboratory is a high-elevation (3220 m a.s.l.) mountaintop research facility in the Park Range in Colorado on top of Steamboat Springs ski resort almost 1500 km from the US west coast. The laboratory marks the location of the Continental Divide and is situated on a 70 km north-south mountain range perpendicular to the prevailing westerly winds, thus providing a clear upwind fetch. The Park Range receives some of the largest precipitation totals in Colorado with most precipitation falling as snow and

typical annual snowfalls at the laboratory in the range of 400–900 cm (Borys and Wetzel, 1997). The laboratory's mountaintop location produces frequent transitions from free tropospheric air to boundary layer and thus allows for time-extended measurements of free tropospheric, in-cloud, and boundary layer air (e.g. Borys and Wetzel, 1997). The site has been used in cloud and aerosol studies for more than 20 years and a considerable depth of knowledge has been acquired on aerosol patterns and interaction of aerosols with clouds (Hindman et al., 1994; Borys and Wetzel, 1997; Lowenthal et al., 2002, 2004).

2.2 Mercury measurements

Atmospheric concentrations of gaseous elemental mercury, reactive gaseous mercury and particulate mercury (GEM, RGM and Hg_P) were measured from 28 April to 1 July 2008. GEM was determined using a Tekran 2537A vapor-phase mercury analyzer. The 2537A instrument collect the air stream on two gold cartridges. GEM is thermally desorbed and detected by cold vapor atomic fluorescence spectrometry at 253.7 nm. Use of dual gold cartridges allowed alternate sampling and desorption, resulting in continuous measurement of GEM on a predefined time base. A precision mass flow meter supplies the 2537A with a sample volume referenced to NTP (Normal Temperature and Pressure: 20°C, 1 atm). Set-up, accuracy, and precision of this instrument have been evaluated previously during field comparisons at an urban/industrial site (Ebinghaus et al., 1999) and a remote marine background location (Schroeder et al., 1995).

Atmospheric mercury speciation was determined by integrating Tekran 1130 and 1135 speciation units with the Tekran 2537A. Both units were positioned on the roof of the Storm Peak Laboratory, at 2 m high, and attached to the pump module and 2537A analyzer by a heated (50°C) umbilical line (10 m long). The Tekran 1130 and 1135 units were configured to collect 1-h RGM and Hg_P samples. During the 1-h sampling period, 5-min GEM samples were continuously quantified by the 2537A analyzer. Ambient air is pumped through a denuder, a quartz filter and a pyrolyzer. Specifically, a potassium

chloride coated quartz annular denuder is housed in the Tekran 1130 unit where RGM is collected (the most probable candidate compounds are $HgCl_2$ and $HgBr_2$). The Tekran 1135 unit consists of a quartz regenerable particulate filter housed in a glass pyrolyzer where Hg_p is collected after passing through a 2.5 μm cutoff impactor (Landis et al., 2002). We set the Tekran 2537A sample flow to 0.8 l min^{-1} and the Tekran 1130 pump flow to 6 l min^{-1}, thus allowing a total flow of 6.8 l min^{-1} during the 1-h time period. However, these flow values set on both instruments corresponds to NTP conditions (293.15 K, 1013.25 mbar). Considering the mean pressure and temperature at Storm Peak Laboratory during our sampling period (278 K, 698 mbar), we actually sampled a total flow of 9.4 l min^{-1}, which allowed a 2.6 μm particle size cutoff by the impactor.

Following 1-h sampling periods, the instruments switch to analysis mode. The system is first flushed with mercury free air to clean out the lines of residual ambient air. The particulate filter is heated to 800°C for Hg_P desorption and quantification as GEM by the Tekran 2537A, followed by heating of the denuder at 500°C for thermal desorption of the collected RGM and quantified as GEM by the analyze. To ensure clean operation, the denuders, denuder module glassware, impactor frits and regenerable particulate filters were replaced and cleaned on a 2–3 weeks basis. To avoid that high humidity corrode of the zero air canisters, the airstream leading into the 1130 pump module during blanks measurement was pumped through a 1102 air dryer Tekran unit.

The Model 2537A was calibrated every 26-h using its internal permeation source. Blanks for the 2537A were measured during each internal calibration cycle and were consistently 0 ng m^{-3}. The manufacturer's reported detection limit for 5 min samples measured with the 2537A of 0.10 ng m^{-3}(http://www.tekran.com/). Detection limit for the 2537A Tekran analyzer was reported by Aspmo et al. (2005) as 0.17 ng m^{-3}. During our study, the detection limit for RGM and Hg_P, calculated as 3 times the standard deviation of the 1130/1135 system blank, was 2 pg m^{-3}.

2.3 Meteorological and chemical measurements

Meteorological instruments used in this study were research grade temperature, pressure, wind speed and direction, and relative humidity sensors (Campbell Scientific, Inc., Met One and Vaisala interfaced to data loggers). Atmospheric tracers included ozone concentrations, aerosol concentrations, and carbon monoxide (CO) concentrations. Aerosol and CO analyzers, however, were not operational continuously, and data were available only 34% and 46% of the measurement period, respectively. O_3 was measured with a Dasibi Ozone Monitor (Dasibi Environmental Corp., Glendale, CA). The instrument has a measurement range of 0.001–1.000 ppm, an automatic zero, and span test. The instrument is calibrated every six months and the UV lamp is replaced if any degradation in signal is observed. Aerosol number concentrations were measured using a stand-alone TSI model 3010 Concentration Particle Counter (CPC) for particles with diameters larger than 10 nm. The TSI CPC instrument is annually sent back to the manufacturer for maintenance and calibrations using National Institute of Standards and Technology (NIST) standards. In addition, the instruments are routinely checked at Storm Peak Laboratory for accurate flow rates. CO concentrations were measured using an isothermal gas chromatograph (Peak Laboratories Model 1 RCP, Mountain View, CA) configured with a reduction gas detector. Its high sensitivity (as low as 10 ppb) and negligible matrix effects from other permanent gases assure reliable detection of ambient and enhanced CO concentrations. The instrument is self-calibrated approximately every 30 min with known standards of CO (54 and 153 ppbv). Meteorological data and aerosol concentration data are uploaded to the Western Regional Climate Center (http://www.wrcc.dri.edu/) database every 5 min. All data were averaged to 2-h mean values which were used for all further analyses.

2.4 Calculations of air mass trajectories

NOAA Hybrid Single-Particle Lagrangian integrated trajectories (HYSPLIT) (Draxler and Rolph, 2003; Rolph, 2003) were calculated for specific dates to determine the

origin of air masses measured at Storm Peak Laboratory. In this study, 10-day back-trajectories were calculated in ensemble forms which calculate 27 trajectories from a selected starting point. Each member of the trajectory ensemble is calculated by offsetting meteorological data by one meteorological grid point (1 degree) in the horizontal (both latitudinal and longitudinal) and 0.01 sigma units (250 m) in the vertical for the selected starting point. HYSPLIT was run with the National Centers for Environmental Prediction's (NCEP) Global Data Assimilation System (GDAS) data set. More information on this data set can be found at http://www.emc.ncep.noaa.gov/gmb/gdas/. The computational height was selected based on the height which most closely represents the common pressure at the lab, 675 mb. The height selected for this data set was approximately 1.8 km a.s.l. which is based on the average height represented by the 1 km grid.

3 Results and discussion

3.1 Spring patterns of atmospheric mercury species

Atmospheric GEM, RGM and Hg_P were investigated at Storm Peak Laboratory during a 64 day period, from 28 April to 1 July 2008. We experienced two short periods with instrument failures (from 26 to 28 May, and from 18 to 21 June). GEM, RGM and Hg_P concentrations, thus collected during 59 days, were compiled into 2-h mean values which correspond to the speciation collection period. A complete time series of the three mercury species is plotted in Fig. 1. The mean GEM concentration and its respective standard deviation was 1.6±0.3 ng m^{-3}. GEM minimum value was 1.2 ng m^{-3} and on eight days GEM levels exceeded 2.0 ng m^{-3}. On two days (15 May and 18 June 2008), GEM values exceeded 3 ng m^{-3} with a maximum value of 5.0 ng m^{-3}). These specifically high pollution events are discussed elsewhere (Hallar et al., in preparation, 2009). GEM concentrations observed at Storm Peak Laboratory during spring 2008 are within the range of values reported from 22 rural sites in the

Northern Hemisphere (i.e. 1.7±0.3 ng m^{-3}) (Valente et al., 2007), and close to an average level of 1.51±0.12 ng m^{-3} reported at the same location during spring 2007 by Obrist et al. (2008).

Mean concentrations and respective standard deviations for RGM and Hg_P were 20±21 pg m^{-3} and 9±6 pg m^{-3} for our entire measurement period. RGM and Hg_P measurements for rural sites in the Western United States have been reported at Yellowstone National Park in summer 2003 (RGM range: <d.l. to 5 pg m^{-3}; Hg_P range: <d.l. to 30 pg m^{-3}) (Hall et al., 2006), in southern New Mexico in 2001–2002 (RGM range: 2 to 25 pg m^{-3}; Hg_P range: 1 to 7 pg m^{-3}) (Caldwell et al., 2006), and at two sites in northern Nevada (RGM : 13±18 and 13±12 pg m^{-3}, Hg_P: 9±7 and 7±8 pg m^{-3}) (Lyman and Gustin, 2008). While Hg_P concentrations at Storm Peak Laboratory were within ranges reported for these rural sites, RGM concentrations were considerably higher. Furthermore, RGM at Storm Peak Laboratory showed several multi-day enhancements periods with maximum level of 50 to 140 pg m^{-3}. Specifically, between 28 April and 1 July we observed eight events of high RGM enhancements (marked in text and figures as RGM enhancement events #1 to #8). RGM enhancement events are defined as occurrences of RGM concentrations higher than the mean level reported for the entire study (i.e. 20 pg m^{-3}, note that the high RGM levels measured on 22 June were not considered an enhancement event since instrument failure prevented a full characterization of this event).

During the eight RGM enhancement events, Hg_P levels were also slightly enhanced, with the exception of event #5. However, significant positive correlation between Hg_P and RGM concentrations was only observed during event #2 (Pearson coefficients r of 0.4, see Table 1). Means, maximums, minimums, and standard deviations of GEM, RGM, and Hg_P for the entire study and for each individual enhancement event are presented in Table 1.

At Storm Peak Laboratory, daytime surface heating can cause air masses enhanced with pollutants to rise from the valley floor, while nighttime air masses are often characterized by cleaner, drier tropospheric air masses (Lowenthal et al., 2002). Such

diel patterns of water vapor concentrations and air pollutants due to local slope flows are typical of high-elevation research stations such as Jungfraujoch (Baltensperger et al., 1997), Sonnblick Mountain Observatory (Seibert et al., 1998), and Mt. Bachelor Observatory (Weiss-Penzias et al., 2006). At Storm Peak Laboratory, diel patterns of atmospheric GEM, however, were only pronounced in the fall and winter season, but not statistically significant in spring months in a previous study (Obrist et al., 2008). Similarly, we did observe daytime increases in aerosols (Fig. 2), water vapor, ozone and CO (not shown) in this study, but not statistically significant differences in GEM between nighttime and daytime concentrations from 28 April to 1 July 2008.

Consistent diurnal trends with RGM concentrations peaking between midday and early afternoon have been previously reported at different rural sites, and were attributed to physical boundary layer movement, ambient photochemistry, or air-surface exchange of mercury (Lindberg and Stratton, 1998; Gabriel et al., 2005; Poissant et al., 2005; Lyman and Gustin, 2008). At Storm Peak Laboratory, RGM also slightly peaked in the afternoon around 03:00 p.m. (Fig. 2). At Mt Bachelor (OR, USA) (Swartzendruber et al., 2006) and Mt Lulin (Taiwan) (Sheu et al., 2009), the only two others high altitude locations where atmospheric mercury speciation has been investigated to our knowledge, RGM peaks were observed at night. These patterns were linked to upslope (anabatic) winds during the day mixing in boundary layer air, and downslope (katabatic) wind which transported high-level, free tropospheric air masses enriched in RGM (see below) to the laboratories at night. Clearly, diel RGM patterns measured at Storm Peak Laboratory – notably much less pronounced compared to Mt Bachelor – showing nighttime minima differed from these previous observations. Moreover, it is of great interest that observed atmospheric RGM levels were mostly unrelated to the diurnal changes in air masses as evident by only minor diel patterns of RGM. In addition, the occurrence of RGM enhancements always lasted for multi-day periods, up to a duration of six days, a starkly different pattern than at Mt. Bachelor where enhanced RGM levels were limited to relatively short nighttime spikes only.

3.2 In situ production and transport of RGM

No relationships between RGM and ozone, aerosols, or CO concentrations were observed over the entire study (Fig. 3) as well as for individual events (data not shown). The lack of correlations of RGM to these common combustion and pollution tracers indicates that high levels of RGM observed at Storm Peak Laboratory were likely not due to anthropogenic pollution from either local sources or from pollution advected by long range transport processes. In fact, if high RGM levels were due to anthropogenic pollution, we would have expected simultaneous increases in RGM and GEM similar to such patterns reported from rural sites which experienced influence of close-by urban pollution (e.g. Yatavelli et al., 2006). In contrast, we observed a clear inverse correlation between GEM and RGM throughout the study (Fig. 4; large panel represents all data from 28 April to 1 July). This inverse relationship becomes even more obvious when considering specifically data considered as RGM enhancement events (insert panel in Fig. 4; 54% of data). Table 1 reports the Pearson coefficients r and sloped between RGM and GEM for each of the eight individual events, with statistically significant linear inverse correlations between RGM and GEM for seven of the eight events (not significant for event #7). The observed inverse correlations between RGM and GEM imply that high RGM levels observed at Storm Peak Laboratory were produced by in situ oxidation processes of GEM. Inverse correlations between RGM and GEM have been reported at Mt Bachelor and in polar regions and are attributed to a direct transformation of GEM to RGM and Hg_p. At Mt Bachelor, a slope near unity (i.e., −0.89) between RGM and GEM was observed during nighttime RGM enhancements, indicating a near mass balance closure between RGM and GEM (Swartzendruber et al., 2006). During the well characterized polar Atmospheric Mercury Depletion Events, on average 40–50% of the converted RGM remains in the air while the remainder is deposited to the snow surface directly as RGM and/or scavenged by fine aerosols (Lindberg et al., 2002; Cobbett et al., 2007). In this study, the significant inverse correlations of GEM and RGM yielded slopes only between −0.07 and −0.18, with an average slope of

−0.10. In other words, observed RGM levels only explained ∼10% of observed GEM depletion. We attribute the obvious lack of mass closure between RGM and GEM in our study to deposition and scavenging of reactive mercury prior to reaching the research station. It is hence likely that Storm Peak Laboratory experienced aged, far-traveled air masses and that the location of the in situ production of RGM occurred in quite some distance to Storm Peak Laboratory, allowing time for considerable scavenging and deposition of RGM. An additional explanation could be surface deposition of reactive Hg species nearby the laboratory.

Figure 5 reports 10-day HYSPLIT back-trajectories for the point of time of maximum RGM levels of each event. Interestingly, all back-trajectories indicate that air masses measured at Storm Peak Laboratory during RGM enhancements events showed source origins over the North Pacific Ocean. We hypothesize that in situ production of RGM likely occur in some distance to our observation station and that scavenging and deposition processes during transport to Storm Peak Laboratory remove a substantial fraction of RGM.

3.3 Possible production and sources of observed high tropospheric RGM levels

Gas-phase reactions with O_3 and OH were the first oxidation mechanisms for atmospheric GEM identified in the troposphere. The chemical lifetime of GEM with respect to oxidation by ozone has been evaluated to 390 days (Hall, 1995) and model simulations have shown (Bergan and Rodhe, 2001) that the determined reaction rate of GEM with O_3 alone cannot explain GEM temporal and spatial variations or the observed diurnal cycles of oxidized mercury (Hedgecock et al., 2005). Oxidation by OH radicals may lead to a lifetime of 115 days for GEM (Sommar et al., 2001; Pal and Ariya, 2004), but theoretical considerations indicate that oxidation of GEM by OH could be slower (Calvert and Lindberg, 2005) and OH oxidation may be insignificant under atmospheric conditions (Goodsite and Plane, 2004; Calvert and Lindberg, 2005). Bromine chemistry may play a major role in the atmospheric oxidation of GEM to reactive mercury species. GEM reacts with both Cl and Br radicals, and kinetics have been

reported of comparable magnitude (Donohoue et al., 2005; Donohoue et al., 2006) or faster with chlorine atoms (Ariya et al., 2002), although, concentrations of Cl radicals are much lower than concentrations of Br radicals (Calvert and Lindberg, 2003). Goodsite et al. (2004) proposed a mechanism for GEM oxidation in the troposphere based on a recombination of GEM with Br radical, followed by the addition of a second radical (Br, OH or I) in competition with thermal dissociation. Fast recombination reaction rates between GEM and Br radical, and elevated levels of Br radicals in the polar marine boundary layer during spring have been proposed sufficient to destroy GEM within a day or two (Ariya et al., 2002, 2004). Raofie and Ariya (2004) also reported a gas-phase reaction of BrO with GEM, but could not exclude the possibility of heterogeneous mechanisms in their experimental set up. However, the homogeneous oxidation of GEM by BrO radicals is considered endothermic (Shepler and Peterson, 2003; Tossel, 2003), and hence probably without importance in the atmosphere. Finally, GEM oxidation to RGM also occurs in the aqueous phase through reaction of GEM with O_3 (Munthe, 1992), OH radicals, (Gardfeldt et al., 2001) and dissolved chlorine (Cl_2) (Lin and Pehkonen, 1998), but due to the low solubility of GEM in water aqueous phase production is considered unimportant.

Unfortunately, our study did not include measurement of halogens, but ozone concentrations were monitored throughout the study. We found, however, no correlations between RGM and ozone levels, neither throughout the study nor specifically during the RGM enhancement events. This is in contrast to results form Mt. Bachelor which showed positive correlation between RGM and ozone during nighttime periods ($p<0.01$; $r = 0.68$). Based on supporting GEOS-Chem modeling, the authors concluded that the oxidation rate of OH and ozone was sufficient to reproduce the mean observed RGM levels, but not to reproduce the magnitude of nighttime RGM enhancements. A lack of RGM to ozone correlation in our study supports these author's notion that additional oxidation mechanisms may contribute to RGM oxidation in the troposphere.

GEM oxidation involving ozone, OH and possibly Br radicals may lead to high RGM levels in the dry, upper troposphere and lower stratosphere as evident by (i) GEM depletion above eight km altitude observed during a research flight (Talbot et al., 2007) and by high levels of aerosol-bound Hg_P in the lower stratosphere (Murphy et al., 2006). Most atmospheric chemistry models have been limited to gas-phase reaction of GEM with O_3 and OH (e.g. Bergan and Rodhe, 2001; Dastoor and Larocque, 2004; Seigneur et al., 2006; Selin et al., 2007; Sillman et al., 2007), and these model simulations, e.g., using the CMAQ model, show that elevated RGM (>200 pg m^{-3}) can form intermittently over the Atlantic Ocean in air masses that have a cloud-free history (Sillman et al., 2007). Similar results were obtained by Selin et al. (2008) with the GEOS-Chem global chemical transport model showing that divalent mercury species could dominate GEM in the upper troposphere and stratosphere. The authors suggest that strong subsidence over the East Pacific and dry conditions result in annual Hg(II) levels of ~125–145 pg m^{-3} over the Southwest US, including our study area (Colorado). Backtrajectories (Fig. 5) indicate some presence of high tropospheric air masses (up to 400 mbar) during RGM events. Further, RGM is correlated to water vapor concentrations during five high-RGM events, and is always strongly related to relative humidity (Table 1 and Fig. 6). Consequently, subsidence of free tropospheric, and these RGM enriched air masses may hence contribute to high RGM levels observed at Storm Peak Laboratory. Such high tropospheric air masses were likely the origin for high nighttime RGM levels observed at Mt. Bachelor, which was supported by positive relationship of RGM to ozone and inverse relationships to CO and H_2O.

However, we can not conclude that high RGM levels observed at Storm Peak Laboratory were exclusively related to the presence of upper tropospheric, or stratospherically influenced, air masses. The backtrajectories (Fig. 5) commonly show the presence of air masses from lower altitudes during RGM enhancements as well. In addition, RGM levels in our study were not related to ozone, were not limited to nighttime periods (and hence katabatic winds), and were not related to high atmospheric pressure (Fig. 6) when large-scale subsidence is most pronounced. We would have expected to see

strong daytime/nighttime differences in RGM levels reflecting different air mass origins (e.g., boundary layer, lower, and higher troposphere), but RGM levels remained constant throughout these enhancement events. We conclude that high RGM levels may be relatively prevalent throughout the troposphere and not be limited to the upper troposphere, at least during springtime over the Western United States.

Based on observed air mass trajectories, one possible source origin of RGM at Storm Peak Laboratory is the North Pacific Ocean. Possibly, halogens released from sea salt aerosols might play a potential role in RGM formation, with strong surface winds in winter and spring causing high sea salt production over the North Pacific (monthly combined level of inorganic bromine species are estimated around 8 pptv in June, Yang et al., 2005). Atmospheric mercury speciation has not been investigated over the North Pacific ocean, but measurements during a ship cruise between Japan and Hawaii showed a distinct diurnal variation in RGM concentrations with maxima at midday, suggesting photochemically driven RGM production in the marine boundary layer (Laurier et al., 2003). Backtrajectories indicate that air masses transport duration from North Pacific to Storm Peak Laboratory is about 5 days, and tropospheric lifetime for RGM is commonly reported in the range of 1–7 days but has been estimated up to 16 days (Selin et al., 2007). Hence, it might be possible that RGM formed over the North Pacific could reach Storm Peak Laboratory, but spatially resolved RGM data (i.e., by aircraft campaigns) will be needed to confirm this hypothesis.

The most constant variable related to high RGM levels in our study, however, is relative humidity (RH, Fig. 6). In fact, the relationship of RGM to RH is so tight that high RGM levels are basically always present when RH drops below ~40%. The relationship of RH to RGM is much more pronounced than correlations to water vapor concentration or to temperature, which suggest that RH directly affects RGM levels and not indirectly through either of the two RH-determining variables. Clearly, low RH may be a sign for the presence of dry, upper tropospheric air masses at the laboratory as found in other stations and discussed above. However, at low RH, RGM were always enhanced, independent of meteorological variables (pressure, wind speed, wind direction, time of the

day) nor chemical tracers (ozone, CO, nor aersol concentrations). This seems a very striking point and could indicate a possible direct effect of RH on RGM production. One possibility could involve for RGM enhancements starting around 40% to 50% RH could be possible heterogenous-phase reactions. Although speculative at this point, surface properties of heterogeneous surfaces such as aerosols may play a role in Hg oxidation or precursor substances, similar to the role of ice surfaces in polar systems (Lindberg et al., 2002) or possibly sulfate aerosols over the Dead Sea (Peleg et al., 2007). Many tropospheric aerosols (e.g. many inorganic salts) are known to be strongly hygroscopic, and hydration of aerosols often lead to very distinct changes in particle morphology, chemistry, and radiative properties (Martin, 2000) as well as phase and size changes (e.g. Hoffman et al., 2004; Wise et al., 2009). The lack of RGM correlations to chemical tracers in our study and the lack of detailed chemical speciation of aerosols, however, does not allow to test this hypothesis, but further studies should be performed to address this possibility for RGM formation in the troposphere.

3.4 Removal processes of RGM

As mentioned above, RGM is to a very high degree controlled by RH of air masses (e.g., Fig. 6), with high RH always leading to low levels of RGM. Figure 1 (bottom panel) also shows that the occurrence of precipitation leads to very strong and immediate drops of RGM to levels close to the detection limit of the analyzer. It is well known that RGM has a high solubility in aqueous phase and that cloud droplets and hydrometeors serve to efficiently scavenging reactive atmospheric mercury forms (Schroeder and Munthe, 1998). This study hence emphasizes that the build-up of high RGM levels in the troposphere is likely limited to the presence of dry air masses.

What seems striking, however, is that the apparent control of RH on RGM levels occurs at low levels of RH which are far below saturation points and hence presence of rain droplets or ice crystals. A possible explanation for this behavior – aside from RH controls on RGM production or presence of dry upper tropospheric air masses as discussed above – is that efficient scavenging processes for RGM may occur not

only by hydrometeors. Clearly, particulates in the atmosphere have been shown to be efficient surfaces for deposition of RGM, e.g. in the polar atmosphere where RGM can exist in the gas phase but is readily sorbed onto aerosols present in the air (Ariya et al., 2004). A possible link to the control of RH could, again, be through the dependence of aerosol size distribution, number concentration, and surface chemistry on RH. For example, liquid coating have been reported for partially deliquesced sea-salt aerosols when RH reach > 57%. If this process is an efficient scavenging pathway, however, RGM reductions should be accompanied by increases in Hg_P. During most RGM enhancement events, however, we observed similar trends for RGM and Hg_P. RGM scavenged on aerosols and hydrometeors, however, might be prone to rapid deposition based on particulate size and mass.

4 Implications

Measurements of atmospheric mercury speciation during spring 2008 at the high-elevation (3220 m a.s.l.) Storm Peak Laboratory showed a very regular occurrence of high RGM levels in the dry troposphere over the Rocky Mountains, Colorado. High RGM levels were not related to pollution events, but showed signs of in situ production, likely in the free troposphere or possibly over the Pacific Ocean. These observations provide evidence that the free tropospheric pool of mercury is enriched in divalent mercury compared to the boundary layer where high RGM levels are mainly related to local and regional pollution. The results support previous modeling studies suggesting that in situ production of RGM could potentially be a large sink for tropospheric mercury, that high RGM levels are not limited to the upper troposphere, and that subsidence of tropospheric air masses can lead to high surface levels and deposition of RGM (Sillman et al., 2007; Selin and Jacob, 2008). Possible mechanism of RGM formation in the free troposphere includes gas-phase production such as oxidation by halogens, but could also include heterogeneous-phase production involving sea-salts or other aerosols, but more detailed chemical characterizations are needed to confirm RGM production pathways.

High levels of RGM over these mountain areas could be of particular concern as high precipitation amounts can lead to high wet deposition rates. Specifically, snowfalls could transfer large amounts of atmospheric Hg(II) to snowpacks. Although photochemical reduction processes in snowpacks can cause partial re-emission of depositions (Faïn et al., 2007), the fate of mercury during snowmelt and runoff and the possible contamination of ecosystems are major issues in alpine regions. For example, fish mercury levels have been reported to exceed health consumption guidelines established by the WHO in several alpine Pyrenees lakes (450 to 2500 m a.s.l.) in France (Blais et al., 2006). In Colorado State, more than 20 lakes are marked with fish consumption advisories due to high mercury levels in fish tissue. This list includes Lake Catamount located 12 miles south of Steamboat Springs (Colorado Department of Public Health and Environment, 2009). Detailed studies are required to assess mercury deposition loads and fate processes of mercury after deposition in rain and snow in mountain areas such as the Rockies Mountains.

Acknowledgements. This research has been funded by the Colorado Department of Health, the NASA EPSCoR Research Infrastructure Development program, and the Desert Research Institute. The study has also benefited from a study funded by the National Science Foundation (ATM 0813690, D. Obrist and M. Luria). We appreciate the assistance from Steamboat Ski and Resort Corporation for continue support of Storm Peak Laboratory and our research projects. We also thank C. Berger, R. Chakrabarty, M. Kaplan, D. Lowenthal, M. Luria, S. Lyman, and H. Moosmüller for valuable discussions and inputs during this manuscript development.

References

Ariya, P. A., Khalizov, A., and Gidas, A.: Reactions of Gaseous Mercury with Atomic and Molecular Halogens: Kinetics, Product Studies, and Atmospheric Implications, J. Phys. Chem. A, 106, 7310–7320, 2002.

Ariya, P. A., Dastoor, A. P., Amyot, M., Schroeder, W. H., Barrie, L. A., Anlauf, K., Raofie, F., Ryzhkov, A., Davignon, D., Lalonde, J. D., and Steffen, A.: The Artic, a sink for mercury, Tellus, 56B, 397–403, 2004.

Aspmo, K., Gauchard, P. A., Steffen, A., Temme, C., Berg, T., Balhmann, E., Banic, C., Dommergue, A., Ebinghaus, R., Ferrari, C., Pirrone, N., Sprovieri, F., and Wibetoe, G.: Measurements of atmospheric mercury species during an international study of mercury depletion events at Ny-Alesund, Svalbard, spring 2003. How reproducible are our present methods?, Atmos. Environ., 39, doi:10.1016/j.atmosenv.2005.07.065, 7607–7619, 2005.

Baltensperger, U., Gaggeler, H. W., Jost, D. T., Lugauer, M., Schwikowski, M., Weingartner, E., and Seibert, P.: Aerosol climatology at the high-alpine site Jungfraujoch, Switzerland, J. Geophys. Res., 102, 19707–19715, 1997.

Bergan, T., and Rodhe, H.: Oxidation of elemental mercury in the atmosphere; constraints imposed by global scale modelling, J. Atmos. Chem., 40, 191–212, 2001.

Blais, J. M., Charpentie, S., Pick, F., Kimpe, L. E., Amand, A. S., and Regnault-Roger, C.: Mercury, polybrominated diphenyl ether, organochlorine pesticide, and polychlorinated biphenyl concentrations in fish from lakes along an elevation transect in the French Pyrenees, Ecotox. Environ. Safe., 63, 91–99, doi:10.1016/j.ecoenv.2005.08.008, 2006.

Borys, R. D. and Wetzel, M. A.: Storm peak laboratory: A research, teaching, and service facility for the atmospheric sciences, Bull. Amer. Meteor. Soc., 78, 2115–2123, 1997.

Caldwell, C. A., Swartzendruber, P., and Prestbo, E.: Concentration and dry deposition of mercury species in arid south central New Mexico (2001–2002), Environ. Sci. Technol., 40, doi:10.1021/es0609957, 7535–7540, 2006.

Calvert, J. G. and Lindberg, S. E.: A modeling study of the mechanism of the halogen-ozone-mercury homogeneous reactions in the troposphere during the polar spring, Atmos. Environ., 37, 4467–4481, doi:10.1016/j.atmosenv.2003.07.001, 2003.

Calvert, J. G. and Lindberg, S.: Mechanisms of mercury removal by O3 and OH in the atmosphere, Atmos. Environ., 39, doi:10.1016/j.atmosenv.2005.01.055,3355–3367, 2005.

Cobbett, F. D., Steffen, A., Lawson, G., and Van Heyst, B. J.: GEM fluxes and atmospheric mercury concentrations (GEM, RGM and Hg-P) in the Canadian Arctic at Alert, Nunavut, Canada (February-June 2005), Atmos. Environ., 41, doi:10.1016/j.atmonsenv.2007.04.033, 6527–6543, 2007.

Colorado Department of Public Health and Environment: Colorado Fish Tissue Study, available at: http://www.cdphe.state.co.us/wq/fishcon/index.html, 2009.

Dastoor, A. P., and Larocque, Y.: Global circulation of atmospheric mercury: a modelling study, Atmos. Environ., 38, doi:10.1016/j.atmosenv.2003.08.037, 147–161, 2004.

Donohoue, D. L., Bauer, D., and Hynes, A. J.: Temperature and pressure dependent

rate coefficients for the reaction of Hg with Cl and the reaction of Cl with Cl: a pulsed laser photolysis-pulsed laser induced fluorescence study, J. Phys. Chem., 109, doi:10.1021/jp0513541, 7732–7741, 2005.

Donohoue, D. L., Bauer, D., Cossairt, B., and Hynes, A. J.: Temperature and Pressure Dependent Rate Coefficients for the Reaction of Hg with Br and the Reaction of Br with Br: A Pulsed Laser Photolysis-Pulsed Laser Induced luorescence Study, J. Phys. Chem., 110, doi:10.1021/jp054688j, 6623–6632, 2006.

Draxler, R. R. and Rolph, G. D.: HYSPLIT (HYbrid Single-Particle Lagrangian Integrated Trajectory) Model Access via NOAA ARL READY Website. NOAA Air Resources Laboratory, Silver Spring, MD, available at: http://www.arl.noaa.gov/ready/hysplit4.html, 2003.

Ebinghaus, R., Jennings, S. G., Schroeder, W. H., Berg, T., Donaghy, T., Guentzel, J., Kenny, C., Kock, H. H., Kvietkus, K., Landing, W., Muhleck, T., Munthe, J., Prestbo, E. M., Schneeberger, D., Slemr, F., Sommar, J., Urba, A., Wallschlager, D., and Xiao, Z.: International field intercomparison measurements of atmospheric mercury species at Mace Head, Ireland, Atmos. Environ., 33, 3063–3073, 1999.

Faïn, X., Grangeon, S., Balhmann, E., Fritsche, J., Obrist, D., Dommergue, A., Ferrari, C., Cairns, W., Ebinghaus, R., Barbante, C., Cescon, P., and Boutron, C.: Diurnal production of Gaseous Mercury in the alpine snowpack before snowmelt, J. Geophys. Res., 112, D21311, doi:10.1029/2007JD008520, 2007.

Friedli, H. R., Radke, L. F., Prescott, R., Li, P., Woo, J. H., and Carmichael, G. R.: Mercury in the atmosphere around Japan, Korea, and China as observed during the 2001 ACE-Asia field campaign: Measurements, distributions, sources, and implications, J. Geophys. Res., 109, D19S25, doi:10.1029/2003jd004244, 2004.

Gabriel, M. C., Williamson, D. G., Brooks, S., and Lindberg, S.: Atmospheric speciation of Southeastern mercury in two contrasting US airsheds, Atmos. Environ., 39, doi:10.1016/j.atmosenv.2005.05.003, 4947–4958, 2005.

Gardfeldt, K., Sommar, J., Stromberg, D., and Feng, X. B.: Oxidation of atomic mercury by hydroxyl radicals and photoinduced decomposition of methylmercury in the aqueous phase, Atmos. Environ., 35, 3039–3047, 2001.

Goodsite, M. E., and Plane, J. M. C.: A Theoretical Study of the Oxidation of Hg° to $HgBr_2$ in the Troposphere, Environ. Sci. Technol., 38, 1772–1776, doi:10.1021/es034680s, 2004.

Hall, B.: The gas oxidation of elemental mercury by ozone, Water Air Soil Poll., 80, 301–315, 1995.

Hall, B. D., Olson, M. L., Rutter, A. P., Frontiera, R. R., Krabbenhoft, D. P., Gross, D. S., Yuen, M., Rudolph, T. M., and Schauer, J. J.: Atmospheric mercury speciation in Yellowstone National Park, Sci Total Environ., 367, 354–366, doi:10.1016/j.scitotenv.2005.12.007, 2006.

Hallar, A. G., McCubbin, I., Obrist, D., Faïn, X., and Rahn, T.: Chemical and aerosol signatures of biomass burning via long range transport observed at Storm Leak Laboratory, in preparation, 2009.

Hedgecock, I. M., Trunfio, G. A., Pirrone, N., and Sprovieri, F.: Mercury chemistry in the MBL: Mediterranean case and sensitivity studies using the AMCOTS (Atmospheric Mercury Chemistry over the Sea) model, Atmos. Environ., 39, 7217–7230, doi:10.1016/j.atmosenv.2005.09.002, 2005.

Hindman, E. E., Campbell, M. A., and Borys, R. D.: A 10-winter record of cloud-droplet physical and chemical-properties at a mountaintop site in Colorado, J. Appl. Meteorol., 33, 797–807, 1994.

Hoffman, R. C., Laskin, A., and Finlayson-Pitts, B. J.: Sodium nitrate particles: physical and chemical properties during hydration and dehydration, and implications for aged sea salt aerosols, J. Aerosol Sci., 35, 869–887, doi:10.1016/j.jaerosci.2004.02.003, 2004.

Landis, M. S., Stevens, R. K., Schaedlich, F., and Prestbo, E. M.: Development and Characterization of an Annular Denuder Methodology for the Measurement of Divalent Inorganic Reactive Gaseous Mercury in Ambient Air, Environ. Sci. Technol., 36, 3000–3009, 2002.

Laurier, F., Mason, R. P., Whalin, L., and Kato, S.: Reactive gaseous mercury formation in the North Pacific Ocean's marine boundary layer: A potential role of halogen chemistry, J. Geophys. Res., 108(D17), 4529, 2003.

Lin, C. J., and Pehkonen, S. O.: Oxidation of elemental mercury by aqueous chlorine (HOCl/OCl-): Implications for tropospheric mercury chemistry, J. Geophys. Res., 103, 28093–28102, 1998.

Lindberg, S. E., and Stratton, W. J.: Atmospheric mercury speciation: concentrations and behaviour of reactive gaseous mercury in ambient air, Environ. Sci. Technol., 32, 49–57, 1998.

Lindberg, S. E., Brooks, S., Lin, C.-J., Scott, K. J., Landis, M. S., Stevens, R. K., Goodsite, M., and Richter, A.: Dynamic Oxidation of Gaseous Mercury in the Arctic Troposphere at Polar Sunrise, Environ. Sci. Technol., 36, 1245–1256, 2002.

Lowenthal, D. H., Borys, R. D., and Wetzel, M. A.: Aerosol distributions and cloud interactions at a mountaintop laboratory, J. Geophys. Res., 107, 4345, doi:10.1029/2001jd002046, 2002.

Lowenthal, D. H., Borys, R. D., Choularton, T. W., Bower, K. N., Flynn, M. J., and Gallagher, M. W.: Parameterization of the cloud droplet-sulfate relationship, Atmos. Environ., 38, 287–292, doi:10.1016/j.atmosenv.2003.09.046, 2004.

Lyman, S. N. and Gustin, M. S.: Speciation of atmospheric mercury at two sites in northern Nevada, USA, Atmos. Environ., 42, 927–939, doi:10.1016/j.atmosenv.2007.10.012, 2008.

Martin, S. T.: Phase transitions of aqueous atmospheric particles, Chem. Rev., 100, 3403–3453, doi:10.1021/cr990034t, 2000.

Munthe, J.: The aqueous oxidation of elemental mercury by ozone, Atmos. Environ., 26, 1461–1468, 1992.

Murphy, D. M., Hudson, P. K., Thomson, D. S., Sheridan, P. J., and Wilson, J. C.: Observations of mercury-containing aerosols, Environ. Sci. Technol., 40, 3163–3167, doi:10.1021/es052385x, 2006.

Obrist, D., Hallar, A. G., McCubbin, I., Stephens, B. B., and Rahn, T.: Atmospheric mercury concentrations at Storm Peak Laboratory in the Rocky Mountains: Evidence for long-range transport from Asia, boundary layer contributions, and plant mercury uptake, Atmos. Environ., 42, 7579–7589, doi:10.1016/j.atmosenv.2008.06.051, 2008.

Pal, B., and Ariya, P. A.: Gas-phase HO center dot-Initiated reactions of elemental mercury: kinetics, product studies, and atmospheric implications, Environ. Sci. Technol., 38, 5555–5566, doi:10.1021/es0494353, 2004.

Peleg, M., Matveev, V., Tas, E., Luria, M., Valente, R. J., and Obrist, D.: Mercury depletion events in the troposphere in mid-latitudes at the Dead Sea, Israel, Environ. Sci. Technol., 41, 7280–7285, doi:10.1021/es070320j, 2007.

Poissant, L., Pilote, M., Beauvais, C., Constant, P., and Zhang, H. H.: A year of continuous measurements of three atmospheric mercury species (GEM, RGM and Hg-p) in southern Quebec, Canada, Atmos. Environ., 39, 1275–1287, doi:10.1016/j.atmosenv.2004.11.007, 2005.

Radke, L. F., Friedli, H. R., and Heikes, B. G.: Atmospheric mercury over the NE Pacific during spring 2002: Gradients, residence time, upper troposphere lower stratosphere loss, and long-range transport, J. Geophys. Res., 112, D19305, doi:10.1029/2005jd005828, 2007.

Raofie, F., and Ariya, P. A.: Product study of the gas-phase BrO-initiated oxidation of Hg-0: evidence for stable Hg^{1+} compounds, Environ. Sci. Technol., 38, 4319–4326, doi:10.1021/es035339a, 2004.

Rolph, G. D.: Real-time Environmental Applications and Display system (READY) Website.

NOAA Air Resources Laboratory, Silver Spring, MD, available at: http://www.arl.noaa.gov/ready/hysplit4.html, 2003.

Schroeder, W. H., Keeler, G., Kock, H., Roussel, P., Schneeberger, D., and Schaedlich, F.: International field intercomparison of atmospheric mercury measurement methods, Water Air Soil Poll., 80, 611–620, 1995.

Schroeder, W. H., and Munthe, J.: Atmospheric mercury - An overview, Atmos. Environ., 32, 809–822, 1998.

Seibert, P., Kromp-Kolb, H., Kasper, A., Kalina, M., Puxbaum, H., Jost, D. T., Schwikowski, M., and Baltensperger, U.: Transport of polluted boundary layer air from the Po Valley to high-alpine sites, Atmos. Environ., 32, 3953–3965, 1998.

Seigneur, C., Vijayaraghavan, K., and Lohman, K.: Atmospheric mercury chemistry: Sensitivity of global model simulations to chemical reactions, J. Geophys. Res., 111, D22306, doi:10.1029/2005jd006780, 2006.

Selin, N. E., Jacob, D. J., Park, R. J., Yantosca, R. M., Strode, S. A., Jaegle, L., and Jaffe, D.: Chemical cycling and deposition of atmospheric mercury: Global constraints from observations, J. Geophys. Res., 112, D02308, doi:10.1029/2006JD007450, 2007.

Selin, N. E. and Jacob, D. J.: Seasonal and spatial patterns of mercury wet deposition in the United States: Constraints on the contribution from North American anthropogenic sources, Atmos. Environ., 42, 5193–5204, doi:10.1016/j.atmosenv.2008.02.069, 2008.

Shepler, B. C., and Peterson, K. A.: Mercury monoxide: A systematic investigation of its ground electronic state, J. Phys. Chem., 107, 1783–1787, doi:10.1021/jp027512f, 2003.

Sheu, G.-R., Lin, N.-H., Wang, J.-L., Lee, C.-T., and Chang, S.-S.: Characterization of speciated atmospheric mercury measured at a high-elevation background station in East Asia: Transport and transformation, 9th International Conference on Mercury as a Global Pollutant, Abstract S06-05, 2009.

Sillman, S., Marsik, F. J., Al-Wali, K. I., Keeler, G. J., and Landis, M. S.: Reactive mercury in the troposphere: Model formation and results for Florida, the northeastern United States, and the Atlantic Ocean, J. Geophys. Res., 112, D23305, doi:10.1029/2006jd008227, 2007.

Slemr, F., Ebinghaus, R., Brenninkmeijer, C. A. M., Hermann, M., Kock, H. H., Martinsson, B. G., Schuck, T., Sprung, D., van Velthoven, P., Zahn, A., and Ziereis, H.: Gaseous mercury distribution in the upper troposphere and lower stratosphere observed onboard the CARIBIC passenger aircraft, Atmos. Chem. Phys., 9, 1957–1969, 2009, http://www.atmos-chem-phys.net/9/1957/2009/.

Sommar, J., Gardfeldt, K., Strömberg, D., and Feng, X.: A kinetic study of the gas-phase reaction between the hydroxyl radical and atomic mercury, Atmos. Environ., 35, 3049–3054, 2001.

Swartzendruber, P. C., Jaffe, D. A., Prestbo, E. M., Weiss-Penzias, P., Selin, N. E., Park, R., Jacob, D. J., Strode, S., and Jaegle, L.: Observations of reactive gaseous mercury in the free troposphere at the Mount Bachelor Observatory, J. Geophys. Res., 111, D24302, doi:10.1029/2006jd007415, 2006.

Talbot, R., Mao, H., Scheuer, E., Dibb, J., and Avery, M.: Total depletion of Hg degrees in the upper troposphere-lower stratosphere, Geophys. Res. Lett., 34, L23804, doi:10.1029/2007GL031366, 2007.

Tossel, J. A.: Calculation of the Energetics for Oxidation of Gas-Phase Elemental Hg by Br and BrO, J. Phys. Chem., 107, 7804–7808, 2003.

Valente, R. J., Shea, C., Humes, K. L., and Tanner, R. L.: Atmospheric mercury in the Great Smoky Mountains compared to regional and global levels, Atmos. Environ., 41, 1861–1873, doi:10.1016/j.atmosenv.2006.10.054, 2007.

Weiss-Penzias, P., Jaffe, D. A., Swartzendruber, P., Dennison, J. B., Chand, D., Hafner, W., and Prestbo, E.: Observations of Asian air pollution in the free troposphere at Mount Bachelor Observatory during the spring of 2004, J. Geophys. Res., 111, D10304, doi:10.1029/2005jd006522, 2006.

Wise, M. E., Freney, E. J., Tyree, C. A., Allen, J. O., Martin, S. T., Russell, L. M., and Buseck, P. R.: Hygroscopic behavior and liquid-layer composition of aerosol particles generated from natural and artificial seawater, J. Geophys. Res., 114, D03201, doi:10.1029/2008jd010449, 2009.

Yang, X., Cox, R. A., Warwick, N. J., Pyle, J. A., Carver, G. D., O'Connor, F. M., and Savage, N. H.: Tropospheric bromine chemistry and its impacts on ozone: A model study, J. Geophys. Res., 110, D23311, doi:10.1029/2005jd006244, 2005.

Yatavelli, R. L. N., Fahrni, J. K., Kim, M., Crist, K. C., Vickers, C. D., Winter, S. E., and Connell, D. P.: Mercury, PM2.5 and gaseous co-pollutants in the Ohio River Valley region: Preliminary results from the Athens supersite, Atmos. Environ., 40, 6650–6665, doi:10.1016/j.atmosenv.2006.05.072, 2006.

Table 1. Summary of the mercury data collected at Storm Peak Laboratory from 28 April to 1 July 2008, including characterization of 8 specific RGM enhancement events. Table includes Pearson's correlation coefficients r between RGM and GEM, RGM and PM, as well as RGM and water vapor concentrations for each individual event. Also given are RGM/GEM regression slopes for each of these events.

		All days	Event #1	Event #2	Event #3	Event #4	Event #5	Event #6	Event #7	Event #8
Starting date and time		4/28/08, 07:00 p.m.	4/28/08, 07:00 p.m.	5/2/08, 11:00, p.m.	5/10/08, 01:00 p.m.	5/16/08, 07:00 p.m.	5/28/08, 05:00, p.m.	6/9/08, 07:00 a.m.	6/13/08, 07:00 a.m.	6/25/08, 05:00 a.m.
Ending date and time		7/01/08, 11:00 a.m.	5/1/08, 03:00 a.m.	5/7/08, 11:00 p.m.	5/12/08, 07:00 p.m.	5/21/08, 09:00 p.m.	6/3/08, 11:00 pm	6/10/08, 11:00 p.m.	6/17/08, 09:00 p.m.	6/28/08, 07:00 p.m.
Duration (hours)			56	118	54	134	150	40	118	86
n^a		760	24	59	27	66	74	21	59	43
Gaseous Elemental Mercury (GEM) ng m^{-3}	Mean±StdDev	1.6±0.3	1.5±0.2	1.5±0.1	1.5±0.1	1.5±0.2	1.5±0.2	1.5±0.2	1.6±0.5	1.5±0.1
	Min	1.2	1.3	1.3	1.4	1.3	1.2	1.2	1.2	1.3
	5.0	1.9	1.9	1.7	2.1	2.0	1.9	5.0	1.9	
Reactive Gaseous Mercury (RGM) pg m^{-3}	Mean±StdDev	20±21	67±23	21±13	21±17	28±27	32±24	36±25	40±21	30±15
	Min	0	7	1	1	0	1	2	2	5
	Max	137	95	58	52	137	84	93	125	71
Particulate Mercury (Hg_P) pg m^{-3}	Mean±StdDev	9±6	13±6	10±3	6±6	9±4	6±4	6±3	16±9	13±5
	Min	0	3	3	1	2	0	3	4	4
	Max	33	32	20	10	22	15	11	31	28
RGM/GEM regression slope			−0.09	−0.08	−0.18	−0.10	−0.09	−0.09	−0.01	−0.07
$r^2_{RGM-GEM}$			**−0.71**	**−0.79**	**−0.86**	**−0.62**	**−0.76**	**−0.62**	0.10	−0.62
r^2_{RGM-PM}			−0.26	**0.44**	0.30	−0.28	**−0.62**	−0.28	−0.06	0.01
$r^{2\,c}_{RGM-WaterVapor}$			–	−0.52	−0.33	**−0.46**	**−0.50**	−0.45	**−0.35**	**−0.48**

[a] n is the number of 2-h sampling periods for GEM, RGM and Hg_P
[b] Correlations significant at $p < 0.01$ are indicated in bold
[c] Water vapor data were not available for event #1

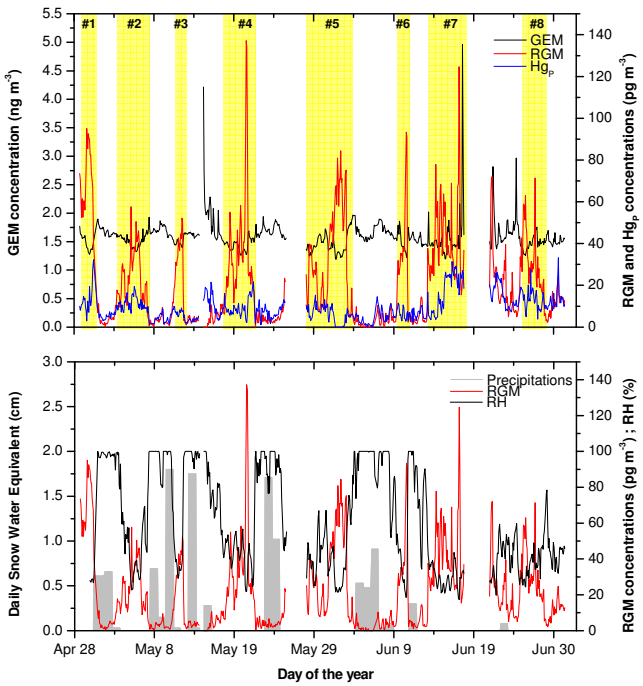

Fig. 1. Time series of GEM, RGM and Hg_P from 28 April to 1 July 2008. Yellow areas highlight the 8 events with enhanced RGM levels (top panel). Records of precipitation (daily cm of snow water equivalent) and relative humidity (RH,%) for the study period are shown in the bottom panel.

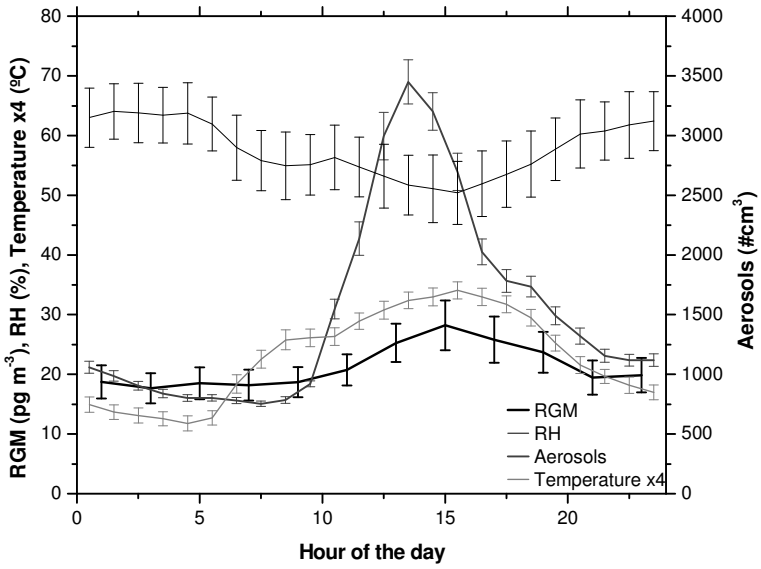

Fig. 2. 24-h, diel patterns of RGM, RH, temperature and aerosol number concentration averaged for the study period. Error bars represent standard errors.

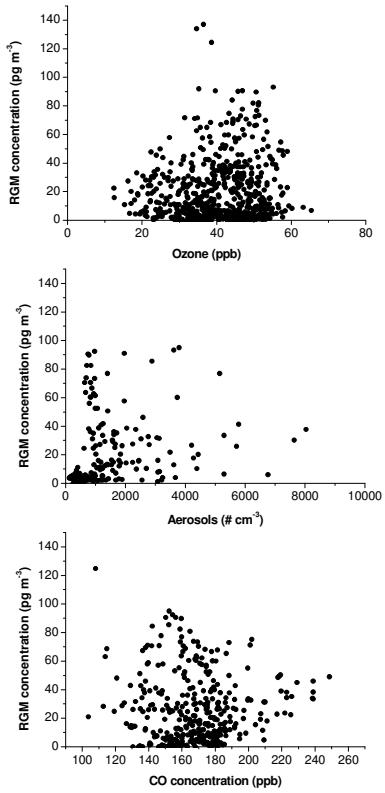

Fig. 3. RGM concentrations as a function of ozone, aerosols, and carbon monoxide for the entire study period.

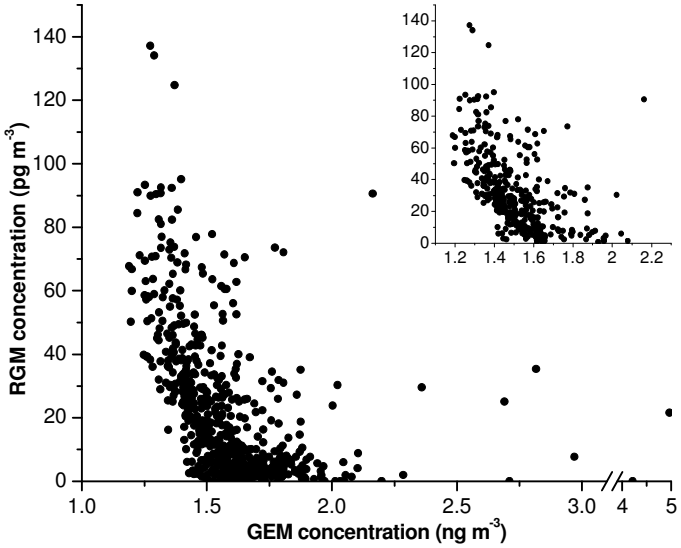

Fig. 4. Correlation between RGM and GEM concentrations for the entire study period. Insert panels show data for the 8 periods characterized as RGM enhancements only (cf. Table 1 and Fig. 1).

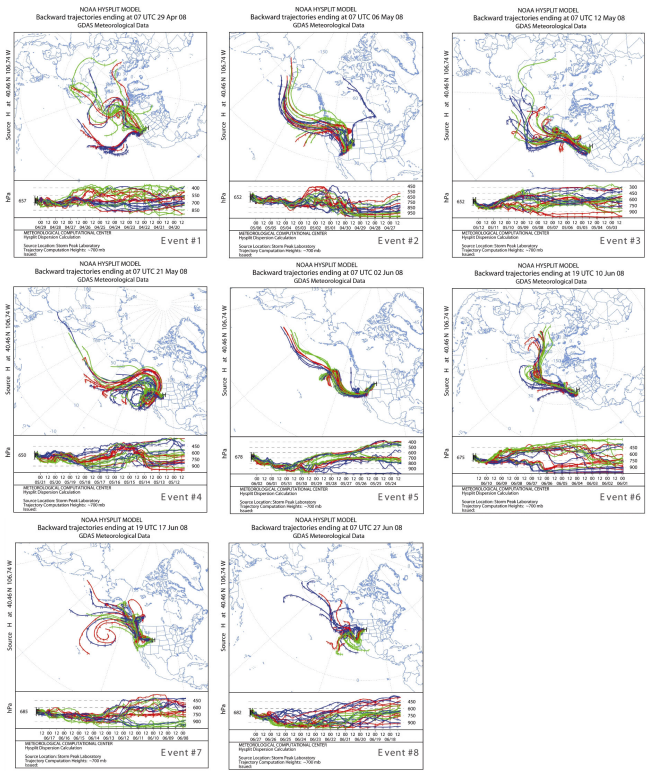

Fig. 5. 10-day HYSPLIT air mass trajectories selected for each RGM enhancement event for the time of at maximum RGM concentration.

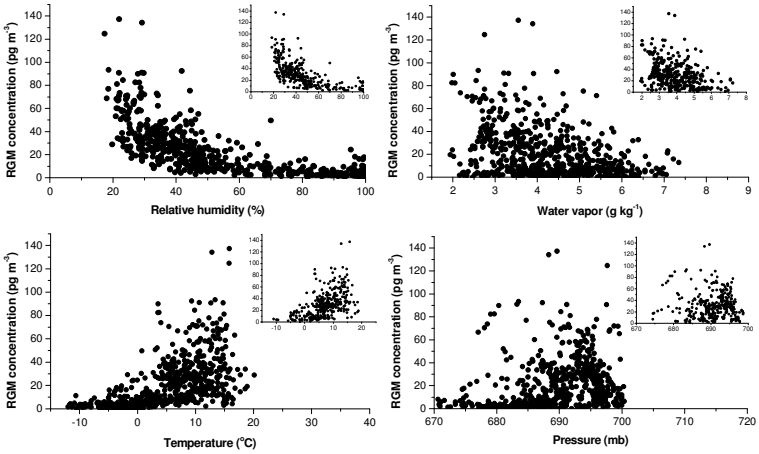

Fig. 6. RGM concentrations as a function of metrological parameters: relative humidity, temperature, water vapor and pressure. Main graphics report data collected during the entire study, and insert graphics show only data collected during events.